

Analysis of a Microsensor Automatic Gain Control Loop ¹

Robert T. M'Closkey
Mechanical and Aerospace Engineering
University of California, Los Angeles
rtm@obsidian.seas.ucla.edu

Alex Vakakis
Mechanical and Industrial Engineering
University of Illinois, Urbana-Champaign
avakakis@uiuc.edu

Abstract

We present the analysis of a nonlinear control system that is used to excite and maintain a specified amplitude of a lightly damped degree of freedom in the Jet Propulsion Laboratory microgyroscope. One- and two-degree-of-freedom models are considered. The analysis suggests that the perturbing effect of an additional weakly coupled degree of freedom does not quantitatively effect the operation of the automatic gain control.

1 Introduction

Vibratory rate sensors require the excitation of a lightly damped degree of freedom. In the Jet Propulsion Laboratory microgyroscope [7,8,9] this is accomplished by applying a sinusoidal potential to the two drive electrodes, denoted D_1 and D_2 in Figure 1. The drive electrodes and sense electrodes (denoted S_1 and S_2) are suspended above four matching electrodes by silicon springs visible in the figure along the x and y axes. The large central post is rigidly attached to the "cloverleaf" formed by D_1 , D_2 , S_1 and S_2 . The post adds inertia to the system which boosts the sensitivity to rotational motion. The electrical potential between the drive electrodes and their respective base electrodes creates an electrostatic force that rocks the cloverleaf assembly about the y -axis. The amplitude of the rocking motion can be maximized by driving the electrodes at the natural frequency of this degree of freedom (referred to as the *drive rocking mode*). If the device is rotated about the z -axis, then the rocking about y is coupled into rocking about the x -axis. The rocking about the x -axis is referred to as the sense mode. In an ideal device, both the drive and sense modes have equal frequencies, since this results in the largest sense axis response. The sense axis rocking velocity is measured by taking the difference of the S_1 and S_2 voltage measurements (which is related to the capacitance between the sense electrodes and their respective base electrodes). Similarly, the drive axis velocity is measured by summing S_1 and S_2 . One of the goals of our research has been to develop high fidelity models of the

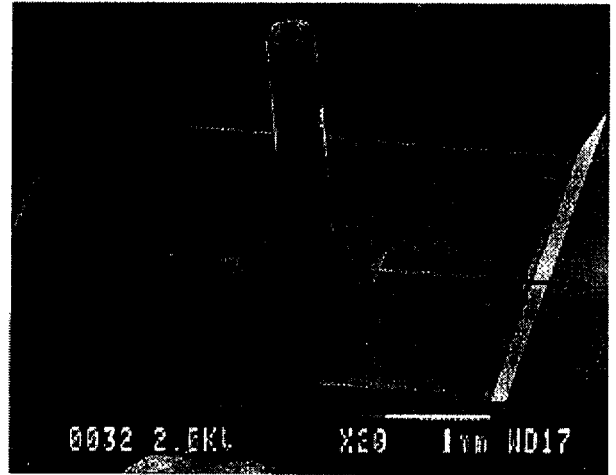


Figure 1: Photo of JPL microgyro (courtesy of T. Tang)

JPL microgyro for the purpose of calibration and compensator design and [5,6] report the results of MIMO model identification experiments. Additional information on microgyroscope technology was recently published in the comprehensive survey [10].

This paper considers the analysis of an *automatic gain control* (AGC) loop that is used to excite the drive rocking mode to a specified amplitude. We study this problem by developing a set of simplified nonlinear equations that describe the application of AGC's to amplitude modulation of an oscillator. The first application of automatic gain control to the JPL microgyro is reported in [7]. In practice there is always some coupling between the drive and sense axis modes. For example, an ARX model fit to input/output data from D_1 to S_1 is shown in the Bode plot in Figure 2. Three distinct modes are present: the two rocking modes of interest and an additional "plunging" mode (the lowest frequency mode). We ignore the plunging mode in the AGC analysis and concentrate on the single- and double-rocking mode case.

The dynamics of the a single oscillator with an AGC is studied in Section 2. Our analysis provides a global picture of the system dynamics and is rigorously justified by the method of averaging. Section 3 studies the non-ideal case when there is coupling between the the drive and sense axes rocking modes via the AGC. The preliminary analysis suggests that the system can

¹This work is supported by Hughes Electronics through UC MICRO Grant No. 96113 and the Jet Propulsion Laboratory through Grant No. PF-433.

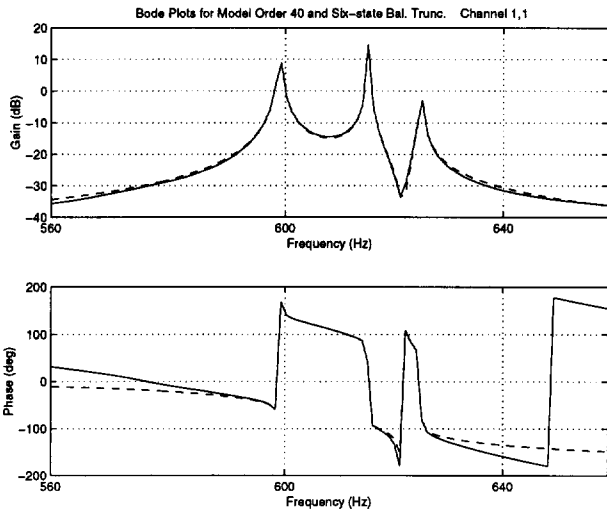
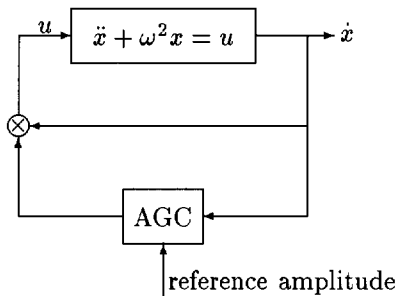


Figure 2: Identified models: 40th-order model (solid) and six-state balanced truncation (dashed)

tolerate a small amount of coupling.

2 Analysis of 1 DOF Model

This section presents the analysis of an AGC loop regulating a single degree of freedom oscillator. The operation of the AGC is intuitive and is explained with the assistance of the following diagram:



In this particular configuration, the velocity of the oscillator is applied to the oscillator input after being multiplied by a gain. The gain is determined by the automatic gain control dynamics: if the desired velocity amplitude is less than the *reference amplitude* then the multiplicative gain is chosen to be negative in order to dampen the oscillations; conversely, if the reference amplitude is larger than the current amplitude then the AGC gain is positive and the “anti-damping” causes the oscillation to grow. This is the essence of a simple automatic gain control. The loop is adaptive in the following sense: if the oscillator natural frequency shifts (which is common in microsensors due to temperature sensitivity), then the AGC loop will track this shift (i.e., the oscillator is always excited at its natural frequency).

The AGC is composed of rectifiers, low-pass filters and comparators and its simplicity makes it attractive for use in microsystem applications. The equations of motion governing a simplified oscillator/AGC are

$$\begin{aligned} \ddot{x} + c\dot{x} + \omega^2 x &= K(r - z)\dot{x} \\ \dot{z} &= \lambda(|\dot{x}| - z), \end{aligned} \quad (1)$$

where x is the oscillator degree of freedom, and z is the state of the low-pass filter which estimates the amplitude of the rectified velocity signal $|\dot{x}|$ (the filter has corner frequency λ). The AGC gain is simply the difference between the reference amplitude, r , and filter state, z , multiplied by the gain K . Integrators may be included to offset the effects of natural damping present in the oscillator (represented by c).

Exact analysis of (1) is difficult because of the nonlinear amplitude detection. Perturbation analysis using periodic averaging, however, leads to simplified nonlinear differential equations. The separation of time scales between the oscillator dynamics and the low-pass filter and AGC gain may be used as the perturbation parameter. The analysis proceeds in several steps. First, a change of time scale and coordinates is performed, then the equations (which are time-periodic) are averaged and, lastly, the approximating system of equations is analyzed.

Time is rescaled by defining τ such that $\tau = \omega t$. Then (1) may be rewritten as

$$\begin{aligned} x'' + \frac{c}{\omega} x' + x &= \frac{K}{\omega} (r - \omega z) x' \\ z' &= \frac{\lambda}{\omega} (|x'| - z), \end{aligned} \quad (2)$$

where ' denotes differentiation with respect to τ . The z variable was also rescaled as $z \rightarrow \omega z$.

A coordinate change transforms the oscillator states x and x' into slowly varying amplitude and phase variables. Define

$$x(\tau) := a(\tau) \cos(\tau + \phi(\tau)), \quad (3)$$

where a and ϕ are the amplitude and phase functions, respectively. Differentiating (3) with respect to τ yields

$$x' = -a \sin(\tau + \phi) + a' \cos(\tau + \phi) - a\phi' \sin(\tau + \phi). \quad (4)$$

The sum of last two terms in this expression is set to zero and is used in determining the equations for a and ϕ :

$$a' \cos(\tau + \phi) - a\phi' \sin(\tau + \phi) \equiv 0. \quad (5)$$

Differentiate (4) once more (keeping in mind (5)):

$$x'' = -a' \sin(\tau + \phi) - a(1 + \phi') \cos(\tau + \phi). \quad (6)$$

Substituting (3), (4) and (6) into the oscillator equation in (2) yields the equation

$$(a' + a(\frac{c}{\omega} - \frac{K}{\omega}(r - \omega z))) \sin(\tau + \phi) + a\phi' \cos(\tau + \phi) = 0. \quad (7)$$

The differential equations for a and ϕ are obtained by premultiplying [(5) (7)]^T by the non-singular matrix

$$\begin{bmatrix} \cos(\tau + \phi) & \sin(\tau + \phi) \\ -\sin(\tau + \phi) & \cos(\tau + \phi) \end{bmatrix}.$$

Simplifying the equations after this step and including the equation for z yields the system

$$\begin{aligned} a' &= \left[\frac{K}{\omega}(r - \omega z) - \frac{c}{\omega} \right] a \sin^2(\tau + \phi) \\ \phi' &= \left[\frac{K}{\omega}(r - \omega z) - \frac{c}{\omega} \right] \sin(\tau + \phi) \cos(\tau + \phi), \quad a \neq 0 \\ z' &= \frac{\lambda}{\omega} (a |\sin(\tau + \phi)| - z). \end{aligned} \quad (8)$$

These equations are exact. To apply averaging [3] we assume

$$\frac{K}{\omega} \propto \frac{\lambda}{\omega} \propto \frac{c}{\omega} \ll 1. \quad (9)$$

Thus the AGC gain K , low-pass filter corner frequency λ , and the damping c are small compared to the oscillator frequency ω , and, in fact, may be reduced proportionally. Since K and λ are parameters that the designer can specify, the analysis really hinges on the requirement that c/ω be sufficiently small. Fortunately, this requirement is not difficult to satisfy because damping in MEMS operating in an evacuated environment is extremely small (quality factors can approach 1×10^5). The quantitative behavior of (8) can be described by the *averaged* system if this condition is satisfied.

The averaged equations are simply,

$$\begin{aligned} \bar{a}' &= \frac{1}{2\omega} [K(r - \omega \bar{z}) - c] \bar{a} \\ \bar{\phi}' &= 0 \\ \bar{z}' &= \frac{\lambda}{\omega} \left(\frac{2}{\pi} \bar{a} - \bar{z} \right). \end{aligned} \quad (10)$$

The averaged variables are denoted with the bar. Note that $\bar{\phi}(t)$ is constant and may be set to zero for the analysis. The performance of the AGC is determined by the response of \bar{a} .

The equilibria of (10) are

$$\begin{aligned} \bar{a}_0 = 0 & \quad \bar{a}_1 = \frac{\pi}{2\omega} \left(r - \frac{c}{K} \right) \\ \bar{z}_0 = 0 & \quad \bar{z}_1 = \frac{1}{\omega} \left(r - \frac{c}{K} \right). \end{aligned}$$

We assume $r > c/K$ since the damping in the microgyro is very small. The Jacobian linearizations at these equilibria are

$$\begin{aligned} D_x f(a_0, z_0) &= \begin{bmatrix} \frac{1}{2\omega}(Kr - c) & 0 \\ \frac{2\lambda}{\pi\omega} & -\frac{\lambda}{\omega} \end{bmatrix} \\ D_x f(a_1, z_1) &= \begin{bmatrix} 0 & -\frac{\pi}{4\omega}(Kr - c) \\ \frac{2\lambda}{\pi\omega} & -\frac{\lambda}{\omega} \end{bmatrix}. \end{aligned}$$

The equilibrium at (a_0, z_0) has one unstable and one stable eigenvalue, however, if $\bar{a}(0) \neq 0$ then the AGC loop is excited.

The eigenvalues of the (a_1, z_1) equilibrium are both stable when $r > c/K$. The eigenvalues of $D_x f(a_1, z_1)$ are

$$\frac{1}{2\omega} \left(-\lambda \pm \sqrt{\lambda^2 - 2\lambda(Kr - c)} \right).$$

In this case, the response of the linearized equations is critically damped with rate of convergence λ/ω when the system parameters satisfy

$$\lambda = 2(Kr - c).$$

The eigenvalues are complex conjugates when $\lambda < 2(Kr - c)$ and oscillations in the amplitude are observed. The design parameters in the AGC are λ and K and these may be used to alter the response the system. Increasing K reduces the effect of damping in the steady state amplitude but produces a more oscillatory response. Note that the response also depends on the reference amplitude r and a larger reference amplitude tends to cause oscillation.

Simulation supports this analysis. For example, a simulation of (10) versus the original equations in (1) is shown in Figure 3. The parameters used in the simulation are $\omega = 10$, $\lambda = 1$, $K = 1$, $r = 1$ and $c = 0.01$. The plot demonstrates that the envelope function, \bar{a} , of the averaged equations has excellent agreement with the amplitude of the oscillator in the complete equations.

A global picture of the \bar{a} - \bar{z} dynamics is desirable. In particular it is of interest to determine the existence of limit cycles. A limit cycle indicates periodic solutions of \bar{a} . This implies the existence of quasi-periodic motion of the oscillator. This situation is undesirable since a constant oscillator amplitude is required for sensor operation. We show that limit cycles cannot exist for the averaged equations.

Recall that the sum of indices of equilibrium points enclosed by a limit cycle must be 1 [4]. This implies that a limit cycle, if it exists, must enclose the equilibrium point (\bar{a}_1, \bar{z}_1) . The closed set $Z = \{(\bar{a}, \bar{z}) : \bar{a} \geq 0, \bar{z} \geq 0\}$ is invariant under the action of (10) because $z' \geq 0$ when $z = 0$ (the vector field points into Z along the \bar{a} axis, for $\bar{a} > 0$). Thus, any limit cycle that passes through part of Z must actually lie entirely in the interior of Z and enclose (\bar{a}_1, \bar{z}_1) . We discount this last possibility by applying Dulac's Criterion [1]. Define

$$f(\bar{a}, \bar{z}) := \frac{1}{2\omega} [K(r - \omega \bar{z}) - c] \bar{a}$$

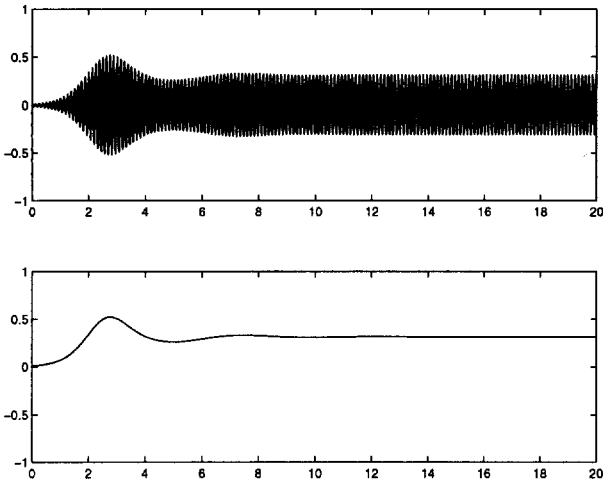


Figure 3: Simulation of $x(t)$ (top plot) and the approximate system $\bar{a}(t)$ (bottom plot).

$$g(\bar{a}, \bar{z}) := \frac{\lambda}{\omega} \left(\frac{2}{\pi} \bar{a} - \bar{z} \right),$$

i.e., $\bar{a}' = f$ and $\bar{z}' = g$, and let $\rho = \bar{a}^m$, where $m \in \mathbb{R}$ is chosen below. Dulac's Criterion states that if the sign of $\frac{\partial(\rho f)}{\partial \bar{a}} + \frac{\partial(\rho g)}{\partial \bar{z}}$ is constant in a simply connected region of the phase space then limit cycles do not exist in the region. Computing this quantity yields

$$\begin{aligned} \frac{\partial(\rho f)}{\partial \bar{a}} + \frac{\partial(\rho g)}{\partial \bar{z}} &= \left[\frac{m+1}{2} \left(\frac{K}{\omega} r - \frac{c}{\omega} \right) - \frac{\lambda}{\omega} \right] \\ &\quad - \frac{m+1}{2} K \bar{z} \bar{a}^m \\ &= -\frac{m+1}{2} K \bar{z} \bar{a}^m \quad \text{when } m := \frac{2\lambda}{Kr - c} - 1 \\ &< 0 \quad \text{on the interior of } Z. \end{aligned}$$

Thus, the interior of Z cannot contain a limit cycle. Further arguments are necessary to determine whether (\bar{a}_1, \bar{z}_1) is globally attractive (except when $\bar{a}(0) = 0$) but the fact that limit cycles cannot occur in this system is encouraging and shows that the AGC is robust to initial conditions (under practical circumstance the AGC loop always excites the oscillator).

3 Preliminary analysis of 2 DOF model

This section contains preliminary analysis of a system with two oscillators and an AGC described by the equations

$$\begin{aligned} \ddot{x} + \frac{c}{\omega} \dot{x} + x &= \frac{K}{\omega} (r - \omega z) (\dot{x} + \epsilon \dot{y}) \\ \ddot{y} + \frac{c}{\omega} \dot{y} + (1 + \epsilon \delta) y &= \epsilon \frac{K}{\omega} (r - \omega z) (\dot{x} + \epsilon \dot{y}) \\ \dot{z} &= \frac{\lambda}{\omega} (|\dot{x} + \epsilon \dot{y}| - z). \end{aligned} \quad (11)$$

Time has been scaled in these equations. The \cdot represents differentiation with respect to τ (the $'$ notation is cumbersome and has been changed back to \cdot).

The motivation for studying this model comes from the inevitable coupling of the two rocking mode degrees of freedom through the AGC. The amount of coupling is determined by $\epsilon \geq 0$. When $\epsilon = 0$, the y -equations decouple from the x - z system. When $\epsilon \neq 0$, \dot{y} "leaks" into the \dot{x} measurement yielding $\dot{x} + \epsilon \dot{y}$. Similarly, the y -equations are forced with an input of order ϵ . The parameter δ represents a detuning of the rocking mode frequencies. Simulations have shown very interesting interaction between the two oscillators in the presence of strong coupling ($\epsilon \approx 0.5$). The analysis of this case is very difficult due to the nonlinearities and high state dimension so we first concentrate on the case when $\epsilon \ll 1$ since the analysis can be developed from the results in Section 2.

The stability of (11) will be studied using regular perturbation series. Assume the following expansions for x , y , and z ,

$$\begin{aligned} x &= x_0 + \epsilon x_1 + \epsilon^2 x_2 + \dots \\ y &= y_0 + \epsilon y_1 + \epsilon^2 y_2 + \dots \\ z &= z_0 + \epsilon z_1 + \epsilon^2 z_2 + \dots \end{aligned}$$

The zeroth order system is

$$\begin{aligned} \ddot{x}_0 + \frac{c}{\omega} \dot{x}_0 + x_0 &= \frac{K}{\omega} (r - \omega z_0) \dot{x}_0 \\ \ddot{y}_0 + \frac{c}{\omega} \dot{y}_0 + y_0 &= 0 \\ \dot{z}_0 &= \frac{\lambda}{\omega} (|\dot{x}_0| - z_0). \end{aligned}$$

The x_0 - z_0 subsystem is the original AGC system considered in (2). The y_0 equation is decoupled from x_0 and z_0 . The approximate steady state solutions for the x_0 - z_0 equations are given by the analysis for the 1 DOF system:

$$x_0(\tau) = \frac{\pi}{2\omega} \left(r - \frac{c}{K} \right) \cos(\tau), \quad z_0(\tau) = \frac{1}{\omega} \left(r - \frac{c}{K} \right). \quad (12)$$

Note that the initial phase is arbitrary in these equations and is taken to be zero. The steady state solution for the y_0 -equation is $y_0(\tau) = 0$.

The first order equations, after *neglecting the nonlinear terms*, are

$$\begin{aligned} \ddot{x}_1 + \frac{c}{\omega} \dot{x}_1 + x_1 &= \frac{K}{\omega} (r - \omega z_0) \dot{x}_1 - K \dot{x}_0 z_1 \\ \ddot{y}_1 + \frac{c}{\omega} \dot{y}_1 + y_1 &= \frac{K}{\omega} (r - \omega z_0) \dot{x}_0 \\ \dot{z}_1 &= \frac{\lambda}{\omega} (\text{sgn}(\dot{x}_0) \dot{x}_1 - z_1). \end{aligned} \quad (13)$$

The signum function is represented by "sgn." The stability of these linearized first order equations is of interest. Note that y_1 is driven by x_0 and z_0 but that the

x_1 - z_1 system does not depend on y_1 . Since the y_1 equation is stable (there is always some damping present in the microgyro so $c > 0$), the stability of (13) is determined by the x_1 - z_1 subsystem which is rearranged to

$$\begin{bmatrix} \dot{x}_1 \\ \ddot{x}_1 \\ \dot{z}_1 \end{bmatrix} = \underbrace{\begin{bmatrix} 0 & 1 & 0 \\ -1 & -\frac{c}{\omega} + \frac{K}{\omega}(r - \omega z_0) & -K\dot{x}_0 \\ 0 & \frac{\lambda}{\omega} \text{sgn}(\dot{x}_0) & -\frac{\lambda}{\omega} \end{bmatrix}}_{A(t):=} \begin{bmatrix} x_1 \\ \dot{x}_1 \\ z_1 \end{bmatrix}.$$

The stability of this linear time-periodic system can be determined by substituting the steady state solutions from (12) and computing the Floquet exponents [2] of $A(t)$,

$$A(t) = \begin{bmatrix} 0 & 1 & 0 \\ -1 & 0 & \frac{\pi K}{2\omega} \left(r - \frac{c}{\omega}\right) \sin \tau \\ 0 & -\frac{\lambda}{\omega} \text{sgn}(\sin \tau) & -\frac{\lambda}{\omega} \end{bmatrix}.$$

The Floquet exponents can be determined for specific parameter cases although it may be possible to derive a perturbation solution for the exponents with the parameters in (9). An analytical solution is desirable since general conditions on the asymptotic stability of the first order equations can then be derived. For now, however, we content ourselves with numerical calculation for specific parameter cases.

Computation of the Floquet exponents, denoted λ_1 , λ_2 , and λ_3 , with the parameters from the simulation in Figure 3 yield,

$$\lambda_1 = 0.69553 + j0.22382 \quad \lambda_2 = 0.69553 - j0.22382 \\ \lambda_3 = 0.99931$$

The magnitudes of the exponents are less than one indicating stability of the first order equations.

This local analysis shows that the AGC continues to operate like the 1 DOF case for small perturbations from the nominal trajectories and that coupling with the y DOF produces a higher order effect on the oscillation of the x DOF. More analysis is required to determine the effect on the starting transients. Simulations support the analysis for small coupling parameter ($\epsilon < 0.2$).

4 Conclusion

The single-oscillator case has been analyzed thoroughly using the method of averaging. Simulations of the averaged equations and the full set describing the oscillator-AGC dynamics shows excellent agreement. The equilibria of the averaged equations were computed and the effect of the AGC parameters on the response of the linearized dynamics was revealed.

The two oscillator case was analyzed for small coupling of the sense axis rocking modes. The results showed that the coupling does not adversely effect the operation of the AGC. More work is required for this case,

however, to determine the range of coupling parameter for which the system functions properly. Additional experimental validation of the results would assist in refining the models and will be reported in future papers as new microgyro prototypes become available for testing.

Acknowledgments: The authors wish to thank Tony Tang, Vatche Voperian, Chris Stell, and Roman Gutierrez at the Jet Propulsion Laboratory, and Dorian Chaloner at Hughes Space and Communications for supporting this research.

References:

1. Andronov, A.A., Vitt, A.A., and Khaikin, S.E., *Theory of Oscillators*, Dover, New York, 1966.
2. G. Birkhoff and G.-C. Rota, *Ordinary Differential Equations*, Wiley, New York, 1989.
3. J. Hale, *Ordinary Differential Equations*, Krieger, Florida, 1980.
4. Jordan, D.W., and Smith, P., *Nonlinear Ordinary Differential Equations*, Oxford Applied Mathematics and Computing Science Series, Oxford University Press, 1987.
5. M'Closkey, R.T., Gibson, J.S., and Hui, J. "Input/output dynamics of the JPL microgyroscope," *1998 IEEE Conf. Dec. Con.*, Dec. 1998, pp. 4328-4332.
6. M'Closkey, R.T., Gibson, J.S., and Hui, J. "Model identification of the JPL microgyroscope," *Proc. ASME*, DSC-Vol. 64, 1998, pp. 801-805.
7. T. Tang, R. Gutierrez, J. Wilcox, C. Stell, V. Voperian, R. Calvet, W. Li, I. Charkaborty, R. Bartman, "Silicon Bulk Micromachined Vibratory Gyroscope," *Solid-State Sensor and Actuator Workshop*, Hilton Head, South Carolina, 1996.
8. T. K. Tang, R. C. Gutierrez, J. Z. Wilcox, C. Stell, and others, "Silicon bulk micromachined vibratory gyroscope for microspacecraft," in *Proc. SPIE*, vol.2810:101-15, 1996.
9. T.K. Tang, R.C. Gutierrez, C.B. Stell, V. Voperian and others, "A packaged silicon MEMS vibratory gyroscope for microspacecraft," *Tenth Ann. Int. Workshop MEMS*, Nagoya, Japan, pp. 500-5, 1997.
10. Yazdi, N., Ayazi, F., and Najafi, K., "Micro-machined Inertial Sensors," *Proceedings of the IEEE*, Vol. 86, No. 8, August 1998, pp. 1640-1659.